ELSEVIER

Materials Science and Engineering B102 (2003) 251–256

MATERIALS SCIENCE & ENGINEERING B

www.elsevier.com/locate/mseb

Temperature behaviour of extended defects in solar grade silicon investigated by photoluminescence and EBIC

Tz. Arguirov [a,c,*], W. Seifert [a,b], M. Kittler [a,b], J. Reif [a,b]

[a] JointLab IHP/BTU, Universitätsplatz 3-4, 03044, Cottbus, Germany
[b] IHP, Im Technologiepark 25, 15236, Frankfurt (Oder), Germany
[c] BTU Cottbus, LS Experimentalphysik II, Universitätsplatz 3-4, 03044, Cottbus, Germany

Abstract

Spatially resolved photoluminescence and EBIC were used to characterise a sample of multicrystalline silicon in the temperature range 80–300 K. The dislocation related lines in the spectrum-D1, D2, D3 and D4 correlate with the total recombination activity measured by EBIC. The temperature dependent EBIC behaviour was utilised to access the contamination level at the dislocations in low quality regions of the sample. The temperature dependence of D1 line shows a maximum at about 150 K. The decrement of D1 peak area upon temperature decreasing below 150 K could be related to the appearance of D3 and D4 lines in the photoluminescence spectra. The peak widths of D1 and D2 show opposite temperature dependence. D1 width decreases and D2 becomes broader upon decreasing temperature. Two additional lines with energies below the energy of band-to-band luminescence were observed together with the D bands at 80 K. They could be related to phonon replication of the band edge luminescence peak and can be seen on FZ-Si too.

Keywords: Photoluminescence; EBIC; Solar grade silicon

PACS numbers: 78.55.Ap; 72.80.Cw; 61.72.Ff

1. Introduction

The room temperature sub-band gap emission of silicon has been subject to increased interest in recent years. The radiation from deep level channels, caused by crystallographic defects has been successfully utilised for nondestructive characterisation of solar grade material [1,2]. The production of high efficient solar cells based on the cost effective multicrystalline silicon requires deeper understanding of the nature of the defects. On the other side the infrared radiation from the defects may provide a means for optoelectronic coupling in silicon based microelectronic chips [3,4].

It was shown recently that dislocations are responsible for regions of low performance in the solar grade materials [5,6]. Their electrical activity is relatively well understood and was found to be related to the degree of contamination (e.g. metals). A model describing the temperature behaviour of dislocation EBIC contrast gives quantitative access to the concentration of the deep-level impurities at dislocations [7]. Despite the well understood recombination activity of the dislocation, the origin of their luminescence is still an open question. It was shown that dislocation related luminescence can be observed only on moderately contaminated dislocations [8,9] with about 1–100 impurity atoms per μm dislocation length. Two of the dislocation related lines discovered in 1976 [10], D3 and D4, can be ascribed to radiative transition (D4) between the shallow one-dimensional bands formed at the dislocation and its phonon replica (D3) [11]. The other two lines, D1 and D2, originate in the vicinity of the dislocations [9]. They were related to self interstitial and metal contamination [9] or to oxygen precipitates at the dislocation [12].

Here we report on dislocation related luminescence in mc-Si, its temperature dependence and spatial distribution.

* Corresponding author. Tel.: +49-355-69-3981; fax: +49-355-69-3985.
E-mail address: arguirov@tu-cottbus.de (Tz. Arguirov).

0921-5107/03/$ - see front matter © 2003 Published by Elsevier B.V.
doi:10.1016/S0921-5107(02)00741-9

2. Experimental

We investigated multicrystalline material produced by edge defined film fed growth (EFG) [5].The material was p type, boron doped to few 10^{15} cm^{-3}. The temperature dependant EBIC measurements were carried out on SEM S360 equipped with cooling stage and picoam-peremeter. For the EBIC measurements an aluminium Schottky contact was prepared at the sample surface.

For the PL measurements the Al contact was removed by etching. The PL spectrum was analysed using a spectrometer equipped with 300 g mm^{-1} grating and liquid nitrogen cooled Ge detector. A laser beam from an Ar ion laser (514 nm) focused to a 100 μm spot at the surface was used as excitation source. The power of the probe beam was 300 mW, resulting in 30 W cm^{-2} excitation.

3. Results

Defect rich areas of the sample can be detected by both photoluminescence and EBIC. Fig. 1 compares two EBIC micrographs (Fig. 1b, d) with two photoluminescence scans (Fig. 1a, c). The measurements were carried out at room temperature (Fig. 1a, b) and at 80 K (Fig. 1c, d). The defect rich areas have higher recombination activity and are dark on the EBIC micrographs. It was shown elsewhere [7] that the temperature behaviour of the contrast can be used to estimate the amount of impurity atoms per unit dislocation length. The defect areas seen on the EBIC micrographs in Fig. 1 show increased contrast at 80 K in comparison to 300 K. Such behaviour is characteristic for dislocations contaminated with 1–100 impurity atoms per μm dislocation length.

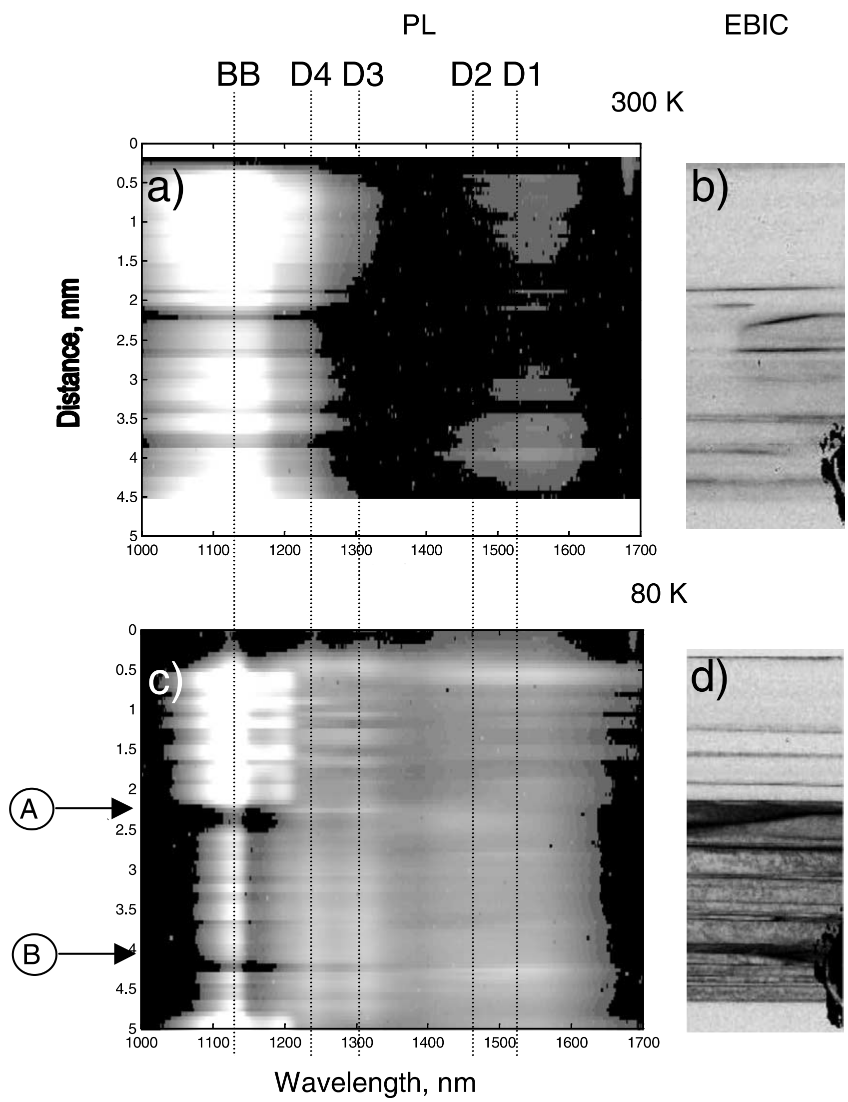

Fig. 1. Comparison between photoluminescence (a and c) scans and EBIC micrographs (b and d) at 300 and 80 K. Luminescence spectra were taken sequentially along a vertical line over the sample. The intensity of luminescent light is given in grey scale with regard to its wavelength and the position on the sample. D lines (D1, D2, D3 and D4) and band to band (BB) luminescence are marked by dashed lines. Single spectra at position A and B are presented in Fig. 2.

EFG silicon is a nearly homogeneous material along the direction of growth. Significant variations in crystalline quality occur perpendicularly to this direction. The essential information about spatial distribution of the radiative centres in our sample could be obtained by scanning perpendicularly to the direction of growth (vertically on the figure). Photoluminescence scans were made at 12 various temperatures between 80 and 300 K. The images in (Fig. 1a, c) were constructed from spectra, recorded at fixed points along the scanning line. They represent the intensity of the luminescence light in grey scale with respect to the wavelength and the position on the sample where the spectrum is measured.

It can be seen that the regions of high recombination activity-dark in EBIC micrographs show a reduction of band-to-band luminescence and increased D band luminescence. The low quality regions reach their highest EBIC contrast at 80 K. The band edge luminescence is strongly reduced there and all D lines are present.

3.1. Spatial distribution of D band luminescence. comparison with EBIC recombination activity

Although there is a similar temperature behaviour of defect sites on the sample, some quantitative differences can be found in between position A at 2.2 mm and position B at 4.1 mm (Fig. 1c). The 80 K spectra at this two positions are given in Fig. 2a and b. The low energy part of the spectra, below the band to band line, was numerically deconvoluted in Gaussian peaks. A prominent difference in the intensity distribution between D1 and D2 in both spectra is found. The intensity of D1 line is much smaller than that of D2 at position A, but both lines have comparable amplitudes at B. D3 and D4 do

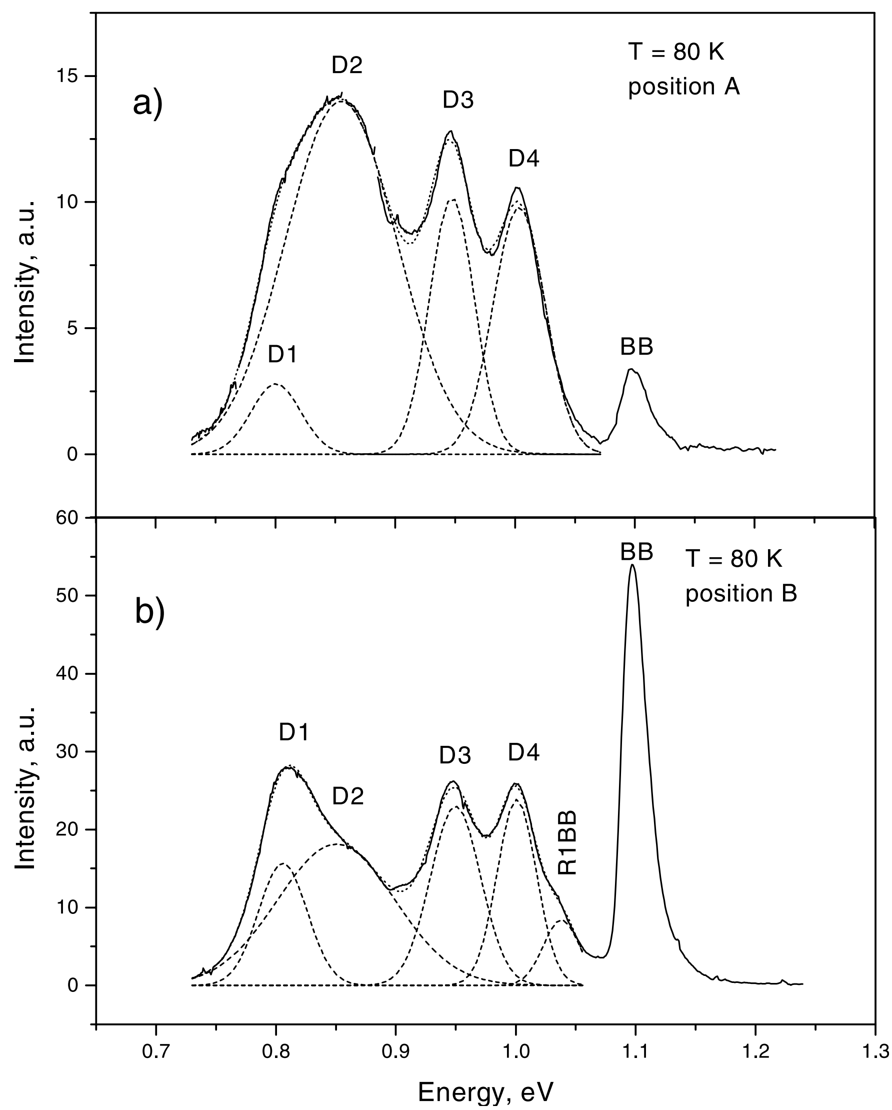

Fig. 2. PL spectra taken at positions A and B (see Fig. 1). The dashed lines are Gaussians, obtained by numerical deconvolution of lower energetic part of the spectrum. The intensity and the width of D3 and D4 stay similar, whereas D1 and D2 peak areas vary strongly. At position A the peak area of D1 is one order of magnitude smaller than D2. The D2 appears always broader than other D lines.

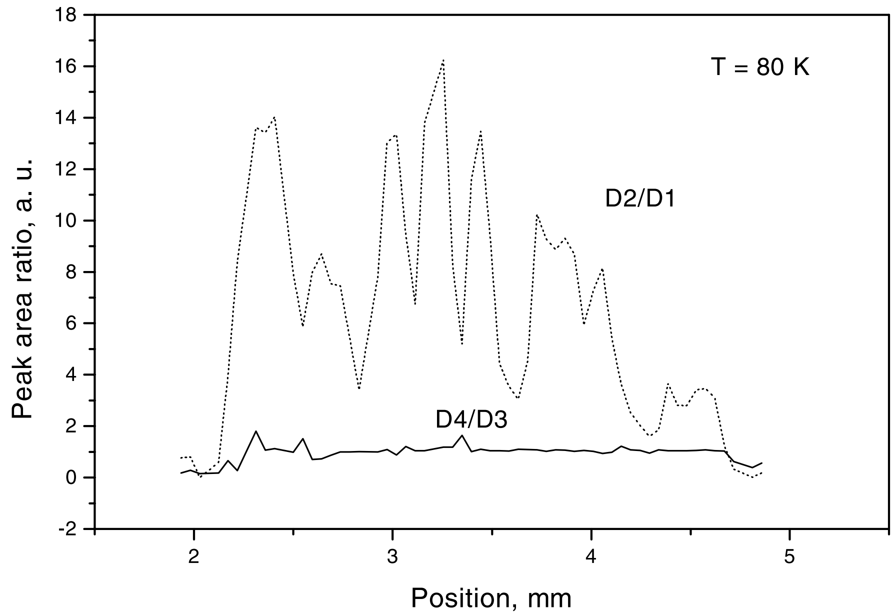

Fig. 3. Spatial distribution of D2/D1 and D4/D3 peak area ratios along the defect part of the sample between position A and B (see Fig. 1) at 80 K. D2/D1 strongly varies, where D4/D3 remains nearly constant.

not differ significantly on both positions. The strong variation of D1 and D2 in comparison with D3 and D4 along the defect rich area between A and B is illustrated in Fig. 3. The figure shows the profile of the peak area ratios D2/D1 and D4/D3. The D2/D1 ratio strongly varies, whether D4/D3 stays almost constant.

It was shown previously [11], that D1 and D2 most probably originate in the dislocation vicinity and D3 and D4 are related to transition at the dislocation core. We suppose that the dislocation vicinities are stronger influenced by the local conditions (dislocation density, material stress) than the dislocations core and that is why there is stronger variance in D1 and D2 trough different regions than in D3 and D4.

3.2. Phonon replication of band edge luminescence

The low temperature spectrum at position A (Fig. 2) shows an additional line at about 1.04 eV. This feature was always observed where band to band luminescence is strong. To find the origin of this line we recorded a spectrum of defect free FZ-Si at the same conditions. Fig. 4 presents the spectrum of FZ-Si together with two spectra taken at high quality and low quality EFG

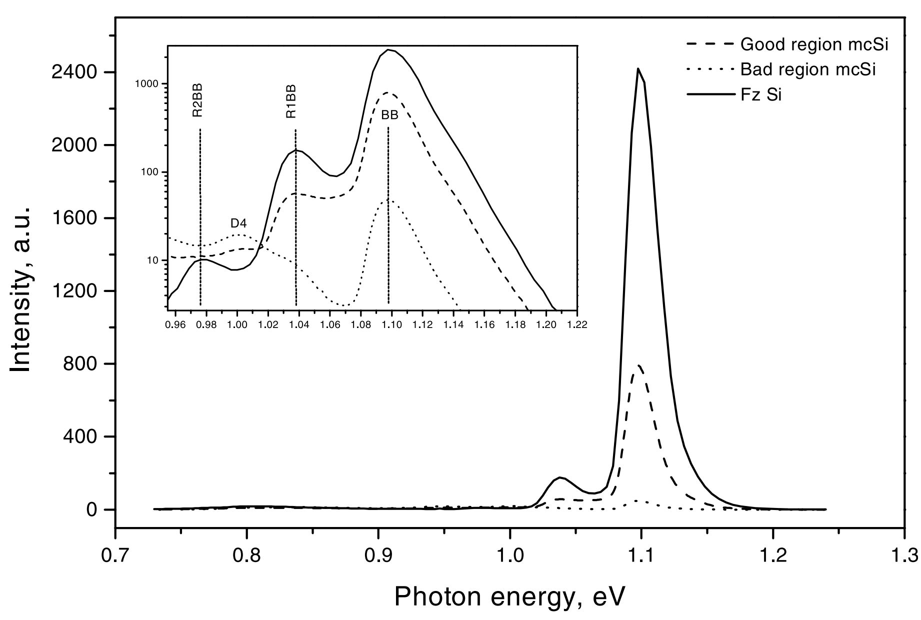

Fig. 4. Comparison of the spectra in high and low quality regions of mc-Si sample with the spectrum of FZ-Si. Two lines R1BB and R2BB are identified as phonon replicas of band edge luminescence.

regions. As expected the intensity of band edge luminescence is highest for FZ-Si. The high quality regions of mc-Si exhibit stronger luminescence than the low quality one. The inset in the figure depicts the intensity of the luminescence in the region close to band edge line in logarithmic scale. The FZ-Si spectrum shows two additional peaks identified as R1BB and R2BB, shifted by about 60 and 120 meV from the band edge line towards lower energies. R1BB can also be seen in the spectrum of high quality region of mc-Si. The D4 line in the spectrum of low quality mc-Si region appears between R1BB and R2BB. The energy shifts with respect to the band edge line correspond to the energies of one phonon for R1BB and two phonons for R2BB. The appearance of these lines in defect free material leads to the conclusion that they are most probably phonon replicas of the band edge emission.

3.3. Temperature dependence of the intensity of the D lines

The temperature quenching of D band intensity has been extensively studied in the literature [3,4,11]. The intensity of all D lines, observed in mc-Si rapidly increases upon lowering the temperature in the interval 300–80 K. At further temperature decrease they remain nearly constant. Fig. 5 depicts peak area dependencies of D bands on temperature for the defect rich region located between A and B (Fig. 1c). At room temperature only D1 is present. Upon decreasing the temperature D2 appears at about 250 K and thereafter D3 and D4 at 190 and 170 K, respectively. D2, D3 and D4 increase upon lowering the temperature, while D1 shows a maximum at about 150 K. The change in the behaviour of D1 could be related to the appearance of D3 and D4. The recombination through D1 becomes lower due to increased recombination through the D3 and D4 centres. It is interesting to note, that the sum of the areas of D1, D3 and D4 lines results in a curve which nearly follows the temperature behaviour of D2.

3.4. Comparison of the temperature behaviour of D1 and D2 peak widths

Fig. 6 depicts the change of the D1 and D2 peak widths versus temperature. The D1 is a broad peak present at room temperature. The D2 appears at about 250 K as a shoulder of D1. Upon decreasing temperature D2 becomes broader and D1 narrower. At about 150 K both lines have equal widths. D2 is twice as

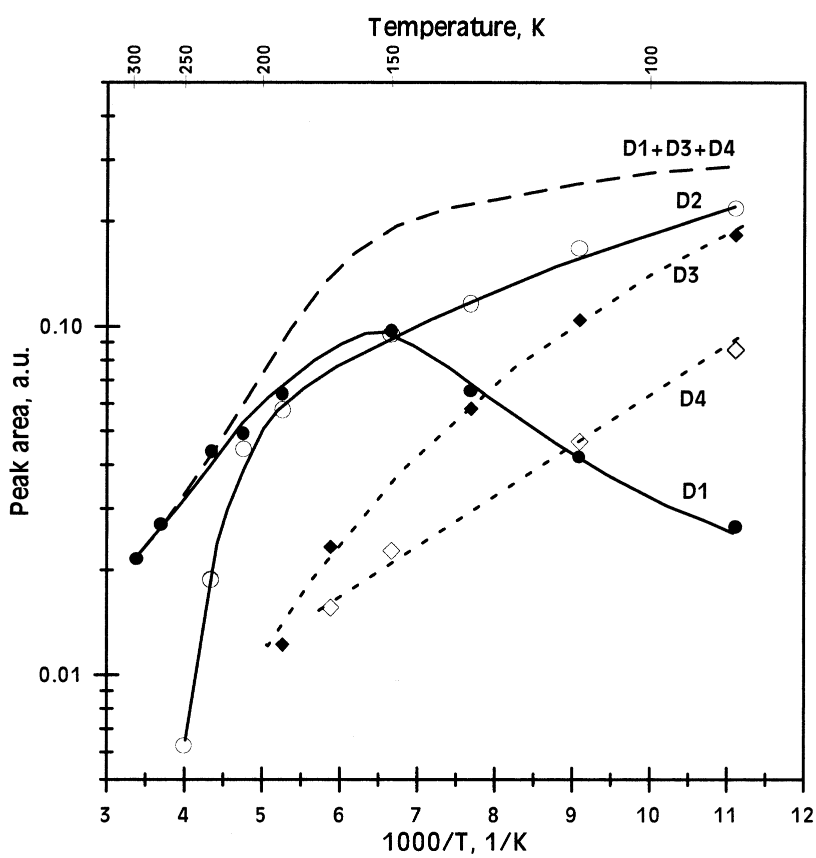

Fig. 5. Temperature dependence of peak areas. The D2, D3 and D4 increase upon lowering temperature. At high temperatures D1 follows the behaviour of D2. However, after appearance of D3 and D4 it starts to decrease upon lowering temperature. The sum of D1, D3 and D4 is shown as dashed line. It is interesting to note that it follows the temperature dependence of D2, nearly.

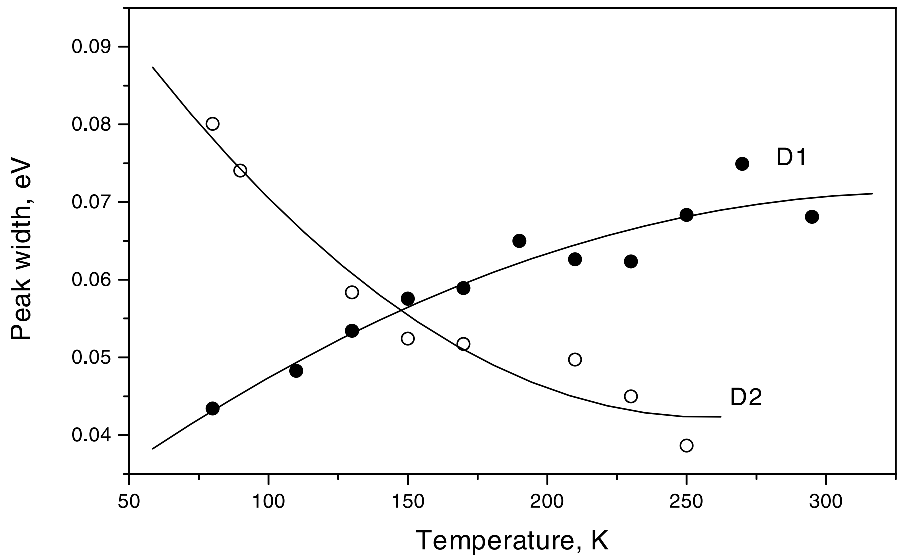

Fig. 6. Temperature dependence of D1 and D2. The D1 peak becomes narrower and the D2 broader upon decreasing temperature. The solid lines are eyeguides.

broader as all other D lines at 80 K (Fig. 3). D1 and D2 change their widths by a factor of about 2 within the entire temperature interval.

4. Conclusion

By comparison between EBIC and spatially resolved PL experiments on multicrystalline EFG-Si we demonstrated that it is possible to establish a correlation between carrier recombination and photoluminescence at dislocation defects. A detailed investigation of the well-known D1, D2, D3, and D4 PL bands confirmed the usual explanation of D3 being a phonon replica of D4, their ratio being independent of the dislocation investigated. In contrast, such image effect could not be found for D1 and D2. Their ratio strongly varies across the sample, and differs even for dislocations looking similar in EBIC. We conclude that D4 and hence D3 originate in the core of the dislocation, whereas D1 and D2 have their origin in the vicinity of the dislocation, thus reflecting a longer range of influence, such as neighbouring dislocations, stress in the sample, etc.

Particularly surprising is the temperature dependence of D1 and D2. While all PL efficiencies, i.e. the integral over the spectral peaks, decreases with increasing temperature, indicating increased quenching, e.g. by electron–phonon scattering, the D1 efficiency below 150 °C grows at about the same rate D3 and D4 diminish. This may point to a delocalisation of the sub-bandgap excitation from the core to the vicinity of the dislocation with increasing temperature. Regarding the opposite temperature dependence of the spectral width of the D1, D2 bands, in particular the narrowing of the D2 line surprises, pointing to less interaction with the environment at higher temperature. Further investigation is needed to better understand this behaviour.

Acknowledgements

The authors would like to thank Dr S. Ostapenko for the fruitful discussions about silicon luminescence, for the submission of samples and for the helpful suggestions and advises on the design of our photoluminescence apparatus.

References

[1] V. Higgs, F. Chin, X. Wang, Solid State Phenomena 63–64 (1998) 421.
[2] I. Tarasov, S. Ostanko, C. Häßler, E.U. Reisner, Mater. Sci. Eng. B 71 (2000) 51.
[3] E.A. Steinman, V.V. Kveder, V.I. Vodovin, H.G. Grimmeiss, Solid State Phenomena 69–70 (1999) 23.
[4] V.V. Kveder, E.A. Steinman, H.G. Grimmeiss, Solid State Phenomena 47–48 (1996) 419.
[5] Y. Koshka, S. Ostapenko, I. Tarasov, S. McHugo, J.P. Kalejs, Appl. Phys. Lett. 74 (11) (1999) 1555.
[6] M. Kittler, W. Seifert, T. Arguirov, I. Tarassov, S. Ostapenko, Solar Energy Mater. Solar Cells 72 (1–4) (2002) 465.
[7] V. Kveder, M. Kittler, W. Schröter, Phys. Rev. B 63 (2001) 115208.
[8] M. Kittler, C. Ulhaq-Boillet, V. Higgs, J. Appl. Phys. 78 (7) (1995) 4573.
[9] V. Higgs, F. Chin, X. Wang, J. Mosalski, R. Beanland, J. Phys. Condens. Matter 12 (2000) 10105.
[10] N.A. Drozdov, A.A. Patrin, V.D. Tkachev, Sov.-Phys. JEPT Lett. 23 (1976) 36.
[11] V.V. Kveder, E.A. Steinman, S.A. Shevchnko, H.G. Grimmeiss, Phys. Rev. B 51 (1995) 10520.
[12] S. Pizzini, M. Guzzi, E. Grilli, G. Borionetti, J. Phys.: Condens. Matter 12 (2000) 10131.